Journal of Applied Polymer Science

The Effect of Depth and Duration of UV Radiation on Polypropylene Modification via Photoinitiation

Yasaman Amintowlieh, Costas Tzoganakis, Alexander Penlidis
Department of Chemical Engineering, Institute for Polymer Research, University of Waterloo, Waterloo, Ontario, Canada N2L 3G1
Correspondence to: C. Tzoganakis (E-mail: costas.tzoganakis@uwaterloo.ca)

ABSTRACT: Linear polypropylene (PP) was modified using UV radiation in the presence of 0.5 wt % of benzophenone photoinitiator to introduce long chain branching (LCB) to the PP backbone. Irradiation was carried out in the solid state and the temperature level was kept below 60°C. The effects of radiation duration and sample thickness on the extent of these branching modification reactions were investigated. Viscoelastic properties, molecular weight, molecular weight distribution, and gel content were determined and compared for runs having different sample thicknesses, irradiated for different times. Comparisons were also conducted with the parent PP and the PP mixed with photoinitiator. It was found that LCB decreased by increasing the thickness of the samples. Conversely, an increase in radiation duration resulted in enhanced LCB but also led to larger gel content in the samples. Based on all these measurements and observations, a mechanism was suggested to explain formation of long chain branches (LCBs) in PP in the solid state via photoinitiation. © 2014 Wiley Periodicals, Inc. J. Appl. Polym. Sci. **2014**, *131*, 41021.

KEYWORDS: crosslinking; irradiation; long chain branching; photochemistry; polyolefins; rheology

Received 5 February 2014; accepted 13 May 2014
DOI: 10.1002/app.41021

INTRODUCTION

Polypropylene (PP) is a commercial polymer with high stiffness and resistance to environmental stress cracking, and solvents. PP applications can be expanded by increasing its melt strength. Increasing melt strength can be achieved by introducing long chain branching (LCB) to the PP backbone. To introduce long chain branches (LCBs) to PP backbone, first, a tertiary hydrogen should be abstracted from the PP backbone. Free radicals generated via peroxide initiator decomposition or high energy radiation, such as electron beam (EB) and gamma radiation, are often responsible for hydrogen abstraction. Combination of a tertiary radical center with another radical center results in formation of branches on the PP backbone. The main difficulty in this process is the tendency of PP macroradicals to degrade via β-scission followed by termination via disproportionation.[1] This mechanism is shown schematically in Figure 1.

Different methods have been used to control the β-scission reaction during PP modification. Using multifunctional monomers (along with peroxide initiators) or radiation (gamma or EB) in the solid state at low temperatures are some of the attempts to stabilize tertiary radical centers.[2–7]

Despite all these advances in modifying the melt strength of PP, the commonly used techniques have several disadvantages. For example, peroxides have toxicity issues related to their use. Moreover, EB and gamma radiation are rather expensive sources of energy and using them involves additional safety issues. Recently, UV radiation under controlled conditions was successfully used to introduce LCB to PP.[8–10] UV radiation is accessible and a rather inexpensive source of energy.

For modification with UV radiation, photoinitiators, such as benzophenone (BPH), have been used. Photoinitiators are activated by UV radiation rather than thermal energy and are less toxic than peroxides. Controlling photoinitiation reactions is easier than peroxide thermal initiation, since temperature can be adjusted without activating the initiator in the former case.

BPH absorbs light in the wavelengths of 215, 254, and 330 nm and becomes excited.[11] In the excited state, it can abstract a hydrogen from the PP backbone and form a macroradical. In more recent work,[10] PP has been modified in the solid state using BPH as photoinitiator. The effect of radiation conditions, such as radiation time, UV lamp intensity, and cooling rate, along with concentration (and type) of photoinitiator on PP modification were investigated. The operating conditions that maximize strain hardening in PP were identified.

One issue that arises during modification of polymers by UV radiation is related to the depth of radiation.[12] It is known that penetration of UV light is limited and this can cause inhomogeneities in LCB (and crosslinking [CL]) of the samples. Chen

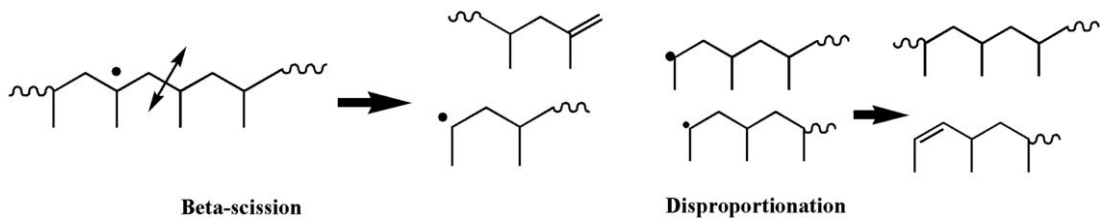

Figure 1. Schematic mechanism for PP degradation.

and Rånby[12] investigated the effect of thickness of polyethylene (PE) samples by analyzing the variation in percent of gel formed and relating it to the thickness of the PE samples.

In this work, the effect of UV penetration depth was investigated by radiating solid PP disks with different thicknesses. Moreover, it is critical to investigate the effect of UV radiation duration along with radiation depth, since radiation time affects the overall extent of the modification process. To investigate the effects of these variables on the degree of modification, disks were prepared with specific thicknesses and radiated for different lengths of time.

MATERIALS AND METHODS

Materials

PP homopolymer (Pro-fax PH 382M) from LyondellBasell with a melt flow rate of 3.5 g/10 min was used. BPH of 99% purity was purchased from Sigma–Aldrich and used as received.

Design of Experiments

To study the effects of UV radiation duration and penetration depth (i.e., sample thickness), three-level factorial design experiments were conducted. Statistical analysis was carried out using Design-Expert 8.0.7.1 software. This design is summarized in Table I (Runs 1–9). Runs 10 and 11 of Table I were used as reference points. Run 10 used a mixture of PP with 0.5 wt % BPH but without any irradiation. Melt mixing for Run 10 was achieved in a batch mixer. Run 11 used simply the parent PP. The experimental results from Runs 10 and 11 were used for comparisons with Runs 1–9.

Table I. Design of Experiments for Three-Level Factorial Design

Run ID	BPH (wt %)	Thickness-A (mm)	Time-B (min)
1	0.5	1	5
2	0.5	1	10
3	0.5	1	15
4	0.5	2	5
5	0.5	2	10
6	0.5	2	15
7	0.5	3	5
8	0.5	3	10
9	0.5	3	15
10	0.5	1	0
11	0	1	0

Preparation Method

PP pellets with 0.5 wt % of photoinitiator were melt mixed in a batch mixer at 190°C and 100 rpm for 8 min. The samples were ground using a Wiley mill (model 1102, Arthur H. Thomas Co.). After grinding, the granules were compression moulded into disks with 25 mm diameter and thickness of 1, 2, and 3 mm at 190°C under an applied force of 4400 *N* for 10–15 min. The disks were irradiated using a Mercury UV lamp (Versa Cure) for varied amounts of time. Radiation was carried out at a distance of 30 cm from the UV light source. Samples were irradiated for 5, 10, and 15 min. During irradiation, pressurized air was used to cool down the area beneath the lamp and the temperature was kept constant at 55°C.

Parallel Plate Rheometry

A stress-controlled parallel plate rheometer (AR2000, TA instruments) was used to measure the rheological properties of the irradiated samples at 190°C. Parallel plates with diameter of 25 mm were used for all tests. Strain sweeps were carried out to identify the linear viscoelastic region during the test (typically less than 1% strain over the whole frequency range). Frequency sweeps were subsequently performed in the range of 0.01–100 Hz at a constant strain of 0.9%. From these tests, storage modulus (G'), loss modulus (G''), complex modulus (G^*), loss tangent (tan δ), and complex viscosity (η^*) were obtained at different angular frequencies (ω).

The validity of the Cox–Merz rule was confirmed, since parallel plate rheometry data (η^* vs. ω) were in agreement with capillary rheometry data (shear viscosity vs. shear rate). Hence, η^* versus ω graphs were used to find the shear thinning index (n), zero shear viscosity (η_0), and relaxation time (λ) of each sample by fitting the Cross model [eq. (1)] using MATLAB (7.11.0 R2010b).

$$\eta^* = \frac{\eta_0}{1+(\omega\lambda)^n} \quad (1)$$

An increase in the zero shear viscosity (η_0) of a run compared to the parent PP indicates higher molecular weight (MW), which can be due to the presence of LCBs. The symbol λ represents the terminal relaxation time whose inverse is related to a characteristic shear rate for departure from the Newtonian plateau. n is the shear thinning index, which is the slope of the shear thinning region in the η^*-ω plots. Long chain branched PP (LCBPP) has larger zero shear viscosity (η_0) and relaxation time (λ) but smaller shear thinning index (n) than linear PP (LPP).[13]

Rheological polydispersity indices were determined using eq. (2–4).[14]

$$\mathrm{PI} = \frac{10^5}{G_c(\mathrm{Pa})} \tag{2}$$

$$\mathrm{ModSep} = \frac{\omega'}{\omega''} \tag{3}$$

$$\mathrm{ER} = C_1 G'_{\ \text{at}\ G''=500\mathrm{Pa}} \tag{4}$$

G_c in eq. (2) is the crossover modulus which is the modulus at which G' and G'' are equal. In eq. (3), ω' and ω'' are the angular frequencies at which G' and G'' are equal to 1000 Pa. In eq. (4), C_1 is the slope of log (G') versus log (G'') curves.

It should be noted that ER is only sensitive to polydispersity of the long time end of the relaxation spectrum, which corresponds to long chains (polydispersity of high MW chains). However, PI and ModSep reflect the polydispersity of shorter chains as well.[14]

Having G' and G'' at different frequencies, the relaxation spectrum can be calculated using eqs. (5) and (6). NLREG is the nonlinear regression software used to calculate the relaxation spectrum [H(λ)]. A broader relaxation spectrum is expected from LCBPP.[15]

$$G'(\omega) = \int_{-\infty}^{+\infty} H(\lambda) \frac{(\omega\lambda)^2}{(1+\omega\lambda)^2} d(\ln(\lambda)) \tag{5}$$

$$G''(\omega) = \int_{-\infty}^{+\infty} H(\lambda) \frac{(\omega\lambda)^2}{(1+\omega\lambda)^2} d(\ln(\lambda)) \tag{6}$$

Gel Permeation Chromatography

High temperature gel permeation chromatography (GPC) [Polymer CHAR (Spain)] was used to determine MW, molecular weight distribution (MWD), polydispersity index (PDI), and intrinsic viscosity [η] of the runs. Refractive index, FTIR, and viscometer detectors were used to characterize each slice of the chromatogram. The GPC setup had three columns in series (PLgel Olexis mixed), and each column was 30 cm long with a diameter of 7.5 mm. 1, 2, 4-trichlorobenzene (TCB) was used as the GPC solvent at 135°C. Each sample of 13–15 mg was dissolved in 9 mL of TCB at 160°C for 90 min. The solutions were visually inspected first for complete dissolution prior to injection. 250 mg/L Irganox 1010 was used as stabilizer.

η_0 of a linear polymer relates to its weight-average MW, which is acquired from GPC measurements, according to the well known relationship shown in eq. (7).[16]

$$\log \eta_0 = \log(K) + a \log \overline{M}_w \tag{7}$$

In eq. (7), K and a are constants; for LPP, log $K = -15.4$ and $a = 3.5$ at 190°C. Equation (7) has been developed for LPP and LCBPP will deviate from this linear relationship (log η_0 vs. $\overline{M}_w$). The magnitude of the deviation can be used to compare structural differences due to the presence of LCBs. For example, a tree-like branching structure results in lower η_0 values than what eq. (7) predicts at the same molecular weight ($\overline{M}_w$), while a star-shaped branching structure results in η_0 values that are larger than what eq. (7) predicts for the same $\overline{M}_w$.[16,17]

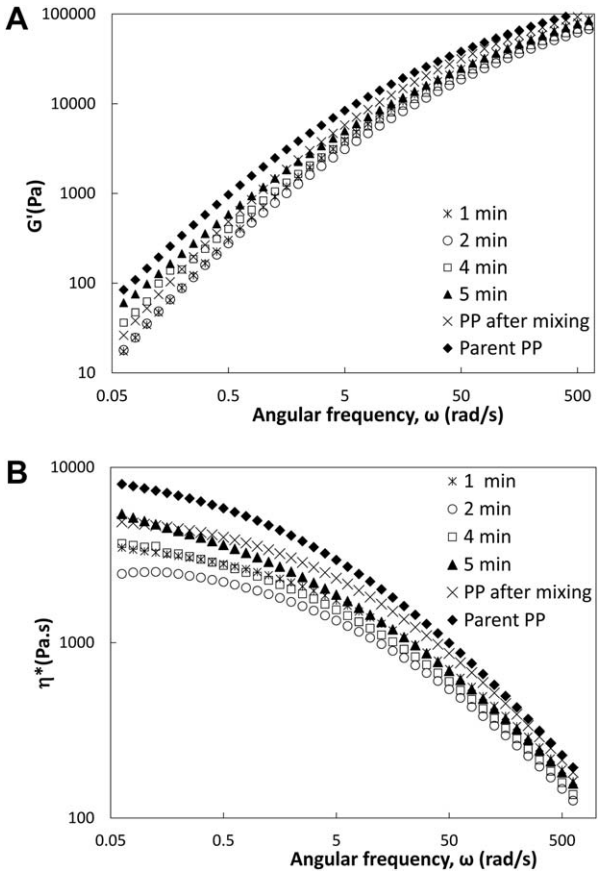

Figure 2. G'(A) and η^*(B) versus ω for 1-mm thick samples which were radiated between 1 and 5 min.

Determination of Gel Content

The percent gel content of selected samples was found by extraction, as described in ASTM D2765-11. Each run was independently replicated and the corresponding standard deviation values were calculated and reported (to be discussed later in Results and Discussion section).

RESULTS AND DISCUSSION

In a previous article,[10] conditions that maximize the LCB level in PP were identified based on rheological properties. In addition, formation of LCB and CL under these conditions was confirmed by extensional rheometry, GPC, and gel content measurements. It was found that to maximize the amount of LCB, samples with 0.5 wt % of BPH should be radiated for 10 min at a lamp intensity of 0.67 W/m^2 in the UVA region at temperatures below 60°C (UVA refers to the wave length range of 320–390 nm where BPH absorbs light). In this article, the main objective is to investigate the effect of time and thickness on the degree of LCB. For this reason, first, preliminarily experiments were conducted to monitor the progress of photomodification with radiation time (from the onset of radiation until formation of branches and/or crosslinks). These results were used to suggest a mechanism for degradation and LCB formation for PP with UV radiation. Figure 2 shows G'(A) and η^*(B) of the runs radiated between 1 and 5 min compared to PP after melt mixing with BPH and the parent PP (Runs 10 and 11

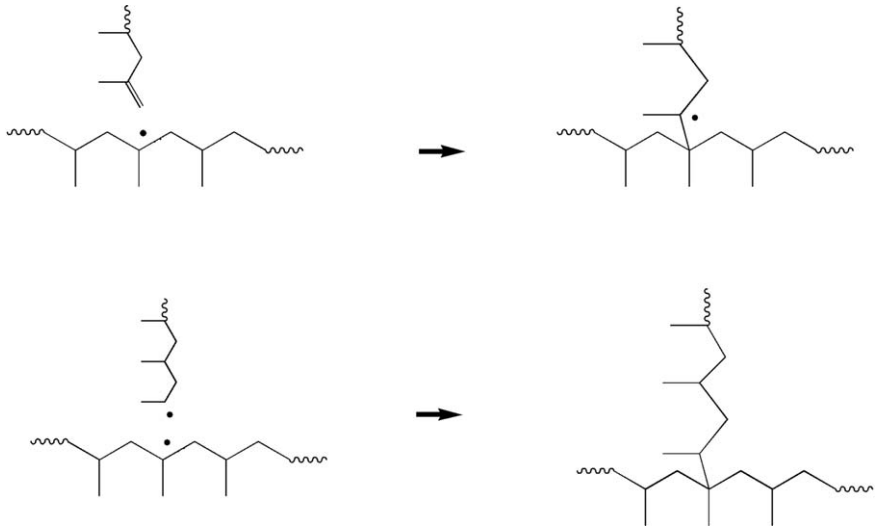

Figure 3. Schematic mechanism for formation of LCB in the PP backbone.

in Table I). All the samples of Figure 2 had a thickness of 1 mm.

In Figure 2(A,B), G' and η^* of PP after mixing (with BPH) are lower than the parent PP due to thermal degradation during the processing in the batch mixer. It can also be seen that G' and η^* decrease after 1 min of radiation and the decrease continues until 2 min from the onset of radiation. This is due to β-scission and degradation of the chains during the first 2 min from the beginning of the reaction (the mechanism is shown in Figure 1). For durations greater than 2 min, rheological properties (G' and η^*) start to increase. This can be attributed to formation of LCB in the samples. Viscoelastic properties continue to increase even after 15 min from the onset of radiation. The effect of radiation time after formation of branches (after 5 min of radiation) is investigated further in the following subsections.

From the above observations, the following mechanism is suggested for formation of LCB in PP via UV radiation (see Figure 3). According to Figure 1, in the first step, excited BPH molecules abstract hydrogens from the tertiary carbon atoms in the PP backbone and form macroradicals. These macroradicals are unstable and undergo β-scission (Figure 1). Due to β-scission reactions, PP chains with terminal double bonds are formed. When the concentration of these chains increases, the probability of reactions between PP macroradicals and chains with terminal double bonds or another PP macroradical also increases (Figure 3). Consequently, LCBs will be formed.

During irradiation, degradation, and LCB happen simultaneously, but as radiation proceeds, LCB will eventually overcome degradation. The validity of this mechanism is corroborated by the experimental observation that degradation is more prominent at the initial stages of radiation (observe the lower η^* and G' levels at the beginning of radiation, as per Figure 2). However, as irradiation proceeds, LCB prevails over degradation, which results in the subsequent increase in η^* and G' (see runs which were radiated for 4 and 5 min in Figure 2).

Effect of Radiation Time and Sample Thickness on Viscoelastic Properties

Viscoelastic properties are known to be sensitive tools for comparison between degrees of LCB (and MWD) of different samples.[18,19]

Figure 4(A,B) shows G' and η^* for Runs 3, 6, and 9, which have the same exposure time to UV (15 min) but different thicknesses (1, 2, and 3 mm, respectively). A lower sample thickness results in larger G' and η^* at low frequencies. This trend is also observed for runs that were radiated for 5 min (Runs 1, 4, and 7) and 10 min (Runs 2, 5, and 8). This is due to the limited depth of radiation for thicker samples. Chen and Rånby[12] found that 1 mm is the critical depth of UV penetration in PE films. Therefore, above this critical thickness, inhomogeneities are expected in CL through the depth of the samples. Since η^* and G' decrease with increasing the thickness of the samples, one can conclude that the critical thickness is either lower than or at 1 mm for disks at the experimental lamp intensity. tan (δ)-G* curves for the same runs are shown in Figure 4(C). The tan (δ)-G* plot is sensitive to the MWD rather than a single MW average.[14] Long chain branched polymers deviate from the linear reference to lower tan (δ) at the same G* values. Due to the thermal degradation of Run 10 (PP after melt mixing), deviation from Run 11 (parent PP) to larger tan (δ) has occurred, which suggests that thermal degradation (at the processing conditions) slightly affects the MWD (narrower MWD than the parent PP). Decreases in tan (δ) versus G* [Figure 4(C)] with a decrease in the sample thickness are mainly due to broadening of the MWD and the larger number of LCBs in the thinner samples.

Figure 5 compares G', η^*, and tan (δ)-G^* plots for the runs with the same thickness (1 mm) but radiated for different amounts of time (5, 10, and 15 min). An increase in radiation time above 5 min increases elasticity (G') [Figure 5(A)] and complex viscosity (η^*) [Figure 5(B)], and broadens the MWD [Figure 5(C)]. This is due to formation of a larger number of branches as the reaction proceeds over time. The same trend

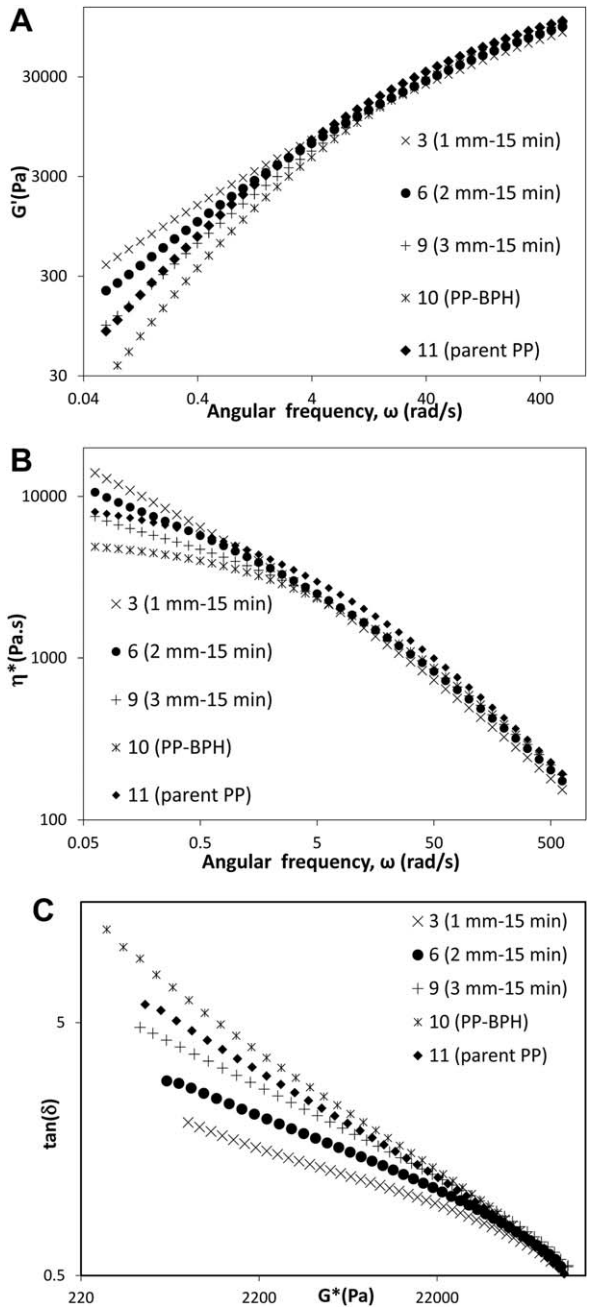

Figure 4. Comparison between viscoelastic properties of the runs with different thickness after 15 min radiation (A) G'-ω, (B) η^*-ω, and (C) tan (δ)-G^*.

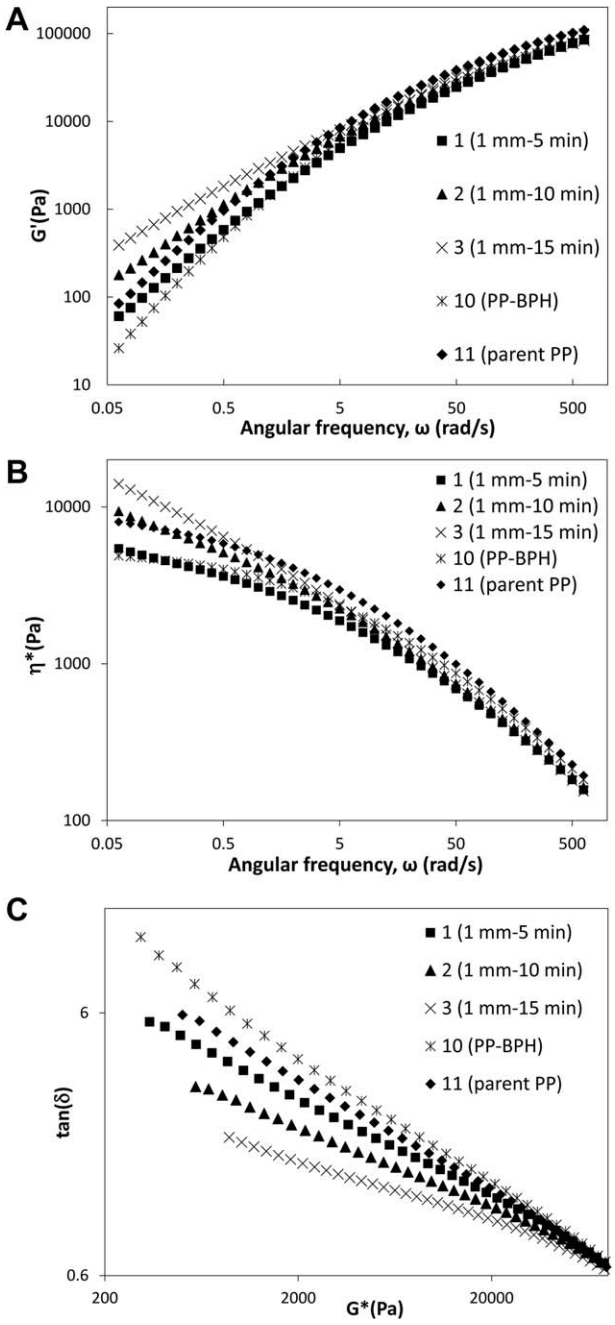

Figure 5. Comparison between viscoelastic properties of the runs with 1 mm thickness with different radiation times (A) G'-ω, (B) η^*-ω, and (C) tan (δ)-G^*.

was observed for runs with 2 mm (Runs 4, 5, and 6) and 3 mm (Runs 7, 8, and 9) thickness that were radiated for varied durations.

The effects of radiation time and depth on the relaxation spectrum, which is an indication of rheological polydispersity, are shown in Figure 6(A,B). Figure 6(A) compares the relaxation spectra of the 1-mm thick samples, which were radiated for 5, 10, and 15 min, respectively. Broadening in the relaxation spectrum occurs after 10 min from the onset of radiation. Increasing the radiation time leads to formation of a bimodal relaxation spectrum, as can be observed for Run 3, which was irradiated for 15 min [Figure 6(A)]. This shows formation of chains with very long relaxation times along with chains with short relaxation times. Since the UV radiation depth is limited, long chain branched polymers with high MW tend to form on the surface of the radiated disks but the molecular properties in the middle of the sample remain unchanged. Consequently, a bimodal relaxation spectrum will most likely result due to differences in relaxation times (and molecular properties) between the sample surface and sample core.

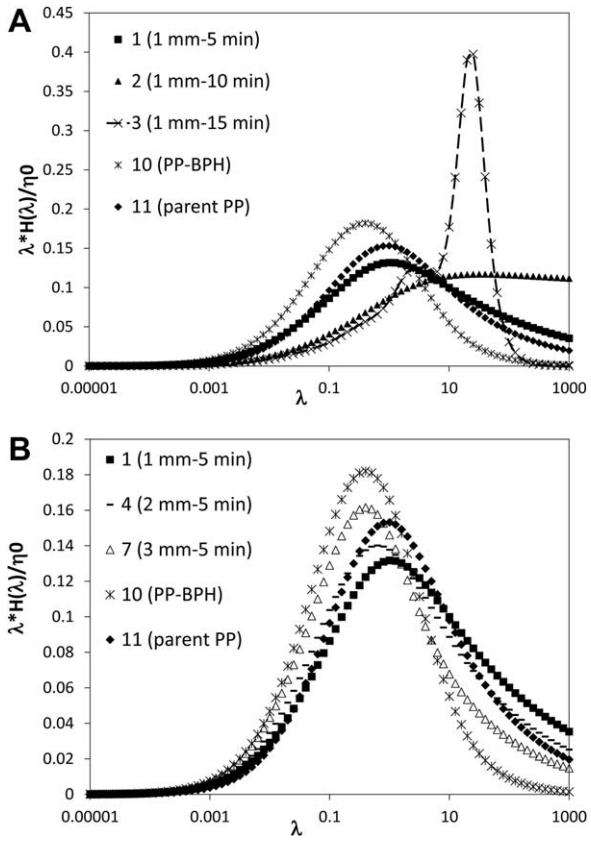

Figure 6. Comparison between relaxation spectra of (A) 1-mm thick samples radiated for different times and (B) samples with different thickness radiated for 5 min.

A broadening in the relaxation spectrum was also evidenced for Runs 4, 5, 6 and 7, 8, 9 (the graphs are not shown here for the sake of brevity), which again confirmed the above mentioned trends (broadening of the relaxation spectrum with radiation time). Broadening of the relaxation spectrum is less pronounced for thicker samples, because the ratio of the surface region to the core region of these (thick) samples is lower. Surface region refers to the outer face of the sample, up to the depth that UV can penetrate, while core region refers to the middle (and lower) part of the sample which UV cannot penetrate.

Scrutinizing now the relaxation spectra of the runs that have the same radiation time reveals that thicker samples have a narrower relaxation spectrum. To compare the effect of thickness on the relaxation spectrum of the runs with the same radiation time, Runs 1, 4, and 7 [Figure 6(B)] are plotted. Runs 2, 5, 8 and Runs 3, 6, 9 showed the same trends; therefore, plots are not shown here again for the sake of brevity. When the radiation time is constant, thinner samples have a broader relaxation spectrum. The relaxation spectrum not only becomes broader by decreasing sample thickness but also shifts to longer times (λ). This is because the number of high MW chains with a high relaxation time is greater in thinner samples.

Viscoelastic constants (η_0, λ, and n) along with rheological polydispersity indices (PI, ModSep and ER) can be found using eqs. (1–4), respectively.

Runs with larger ER values indicate a broader distribution of the high MW chains. PI and ModSep are polydispersity indicators for the shorter chains. An increase in PI and a decrease in ModSep indicate broadening of the MWD[14] It is expected that LCBPP have a larger ER due to the presence of high MW chains and broader MWD. An increase in PI and decrease in ModSep are also expected due to broadening of the MWD during UV modification. Moreover, formation of LCB results in a larger η_0 and λ, and a lower shear thinning index (n).

η_0, λ, n, and polydispersity indices of the runs are summarized in Table II. It can be seen that all radiated Runs (1–9) have larger η_0, λ, and ER, and lower n values compared to Run 10, which is PP after melt mixing with BPH.

Comparison between Runs 1, 2, and 3 shows that longer exposure time to UV results in larger η_0, λ, and lower n values, as expected from the η^* versus ω graphs (Table II and Figure 5). This trend is also observed for the 2 mm (Runs 4, 5, and 6) and 3 mm (Runs 7, 8, and 9) samples. Conversely, an increase in the thickness of the samples limits UV light penetration and subsequently results in lower η_0, λ, and higher n at the same exposure times (compare Runs 1, 4, and 7, or 2, 5, and 8, or 3, 6, and 9). This is because all these viscoelastic constants are indicators of an average property within the sample. Therefore, due to the limited UV penetration in the samples, formation of LCB or CL is not uniform in thicker samples.

The data points presented in Table II were analyzed next with the Design-Expert software. It was found that the time-thickness interaction is significant for all responses except for ER and n. Time-thickness interaction plots for η_0 and ModSep are shown in Figures 7 and 8, respectively. In these figures, the full, dotted and dashed lines show the statistical fit at 5, 10, and 15 min of radiation, respectively, while the square, triangle, and cross symbols represent the actual data points corresponding to the 1, 2, and 3 mm samples, respectively. The interaction plots for λ and PI are not shown again for the sake of brevity but the trends were the same as with η_0 and will be discussed below.

For all these responses, the effect of thickness is not as pronounced at low radiation times. However, at longer radiation times, an increase in thickness results in a decrease in η_0, λ, and PI. At high radiation times, ModSep shows the opposite trend and correlates directly with the time-thickness interaction (i.e., an increase in thickness results also in an increase in ModSep). This is expected as ModSep has an inverse relation with MWD (unlike PI and ER, an increase in ModSep indicates a narrower MWD). In the same way, the effect of time is more significant when the thickness of the samples is low. The increase in η_0, λ, and PI, and decrease in ModSep, of the runs is less pronounced for thicker samples. This shows that an increase in MW and broadening of the MWD due to formation

Table II. Viscoelastic Properties of the Runs

Run #	Thickness (mm)	Time (min)	η_0 (Pa.s)	λ (s)	n	PI	ModSep	ER
1	1	5	6,620	1.5	0.50	4.22	3.37	1.46
2	1	10	16,700	12.3	0.47	4.78	2.94	1.95
3	1	15	39,900	71.1	0.48	7.46	2.31	3.27
4	2	5	6,730	0.96	0.51	3.56	3.69	1.23
5	2	10	9,400	2.53	0.48	3.72	3.44	1.42
6	2	15	17,400	10.9	0.47	4.30	3.04	2.12
7	3	5	6,130	0.46	0.55	3.08	4.01	1.03
8	3	10	6,980	0.82	0.52	3.26	3.81	1.28
9	3	15	9,980	2.37	0.49	3.52	3.53	1.39
10	1	0	5,290	0.30	0.60	3.43	3.94	0.82
11	1	0	9,325	0.79	0.57	3.63	3.64	1.27

of LCBs are more significant at low thickness and with increasing radiation time.

Effect on MW and MWD

In this section, the effects of sample thickness and radiation time on MW, MWD, and intrinsic viscosity [η] of the samples are investigated.

Number average ($\overline{M}_n$), weight average ($\overline{M}_w$), z average ($\overline{M}_z$), and PDI values from all runs are summarized in Table III. In Table III, when the thickness is low, the effect of radiation time is more significant. Comparing the 1-mm thick samples (Runs 1, 2, and 3), it can be inferred that longer radiation times result in larger average MWs (in principle) and PDI; however, these changes are less pronounced when the thickness increases (2 and 3 mm runs). The MW trends will be revisited shortly.

As expected, Run 3 has the highest PDI due to the larger amount of LCB. Run 3 has the highest radiation time and the lowest thickness, and our results from rheological measurements (η_0, λ, n, ER, and relaxation spectra) have suggested that as thickness decreases and radiation time increases, more LCBs will be formed in the sample. This formation of a greater number of LCBs is translated in greater PDI values (broadening of the MWD toward the high MW end).

Having the weight average MW ($\overline{M}_w$) values from GPC, η_0 can be calculated using eq. (7). Comparing the calculated η_0 [eq. (7)] and η_0 from the viscoelastic measurements (Cross model), one can make inferences[16,17] about the type of the LCBs (see also the GPC section under Materials and Methods). Figure 9 shows these calculated η_0 and measured η_0 [eq. (1)] values versus $\overline{M}_w$ for all experimental runs.

Runs 2, 3, 5, 6, and 9 are above the linear reference [eq. (7)], which indicates that the LCBs in these runs are possibly star-shaped. In the 1-mm thick samples (Runs 1, 2, and 3), radiation for 5 min does not cause a significant deviation above the linear reference, whereas after 10 min of radiation $\overline{M}_w$ decreases (Table III), but η_0 increases (Table II). Increasing the radiation time to 15 min results in an increase in both MW and η_0. Samples with thickness of 2 mm (Runs 4, 5, and 6) also exhibit a similar trend. The suggested reason for this trend is degradation, which happens at the onset of radiation and then in parallel to the LCB reactions. Degradation results in a decrease in MW; however, a subsequent formation and increase in the amount of LCBs can compensate for the effect of initial degradation. Radiation for 5 min does not cause significant changes in the MW of the samples (Runs 1 and 4). After 10 min, and despite formation of LCBs (η_0 is above the linear reference), the

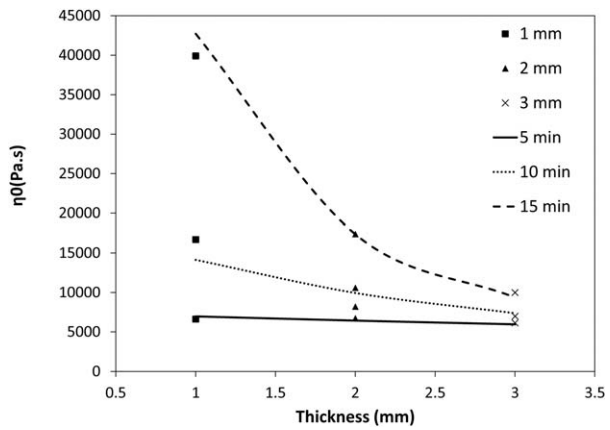

Figure 7. Effect of the time-thickness interaction on zero shear viscosity (η_0).

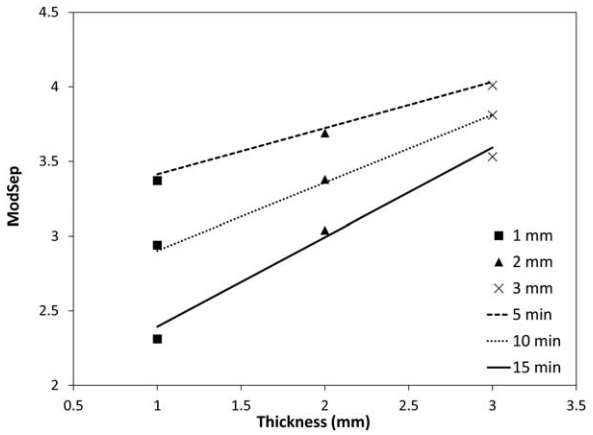

Figure 8. Effect of the time-thickness interaction on ModSep.

Table III. Molecular Weight Averages and PDI of the Radiated Runs Along with Melt Mixed and Parent PP

Sample ID	Thickness	Radiation time (s)	$\overline{M}_n$(kg/mol)	$\overline{M}_w$(kg/mol)	$\overline{M}_z$(kg/mol)	PDI
1	1	5	69.2	320.2	908.9	4.6
2	1	10	43.1	259.1	904.2	6.0
3	1	15	36.5	377.1	1,331.8	10.3
4	2	5	71.8	329.6	650.2	4.6
5	2	10	53.0	214.5	502.9	4.0
6	2	15	67.5	357.3	919.3	5.3
7	3	5	77.7	310.9	676.7	4.0
8	3	10	76.3	330.4	582.4	4.3
9	3	15	66.8	277.9	700.8	4.2
10	1	0	75.0	317.9	591.2	4.2
11	1	0	78.4	361.4	714.8	4.6

effect of degradation on the MW is still more dominant than that of LCB (Runs 2 and 5). In other words, the population of LCBs is not high enough to compensate for initial degradation effects on $\overline{M}_w$. An increase in $\overline{M}_w$ is observed after 15 min from the onset of radiation, when the amounts of long chain branched (and crosslinked) molecules are large. This subsequently results in an increase in $\overline{M}_w$ and deviation of η_0 above the linear reference.

For the 3-mm thick samples, the decrease in $\overline{M}_w$ (Table III) and increase in η_0 (Table II) were only evident after 15 min from the onset of radiation. This is because the MW of the thick samples is not as affected due to UV penetration limitations, and therefore, the average molecular properties of the samples can remain unchanged even after long radiation times.

To compare the MWDs of the runs with 1 mm thickness at different radiation durations, the MWDs are summarized in Figure 10(A). Figure 10(B) contrasts the MWDs of the runs with different thicknesses that were exposed to UV for 15 min. In Figure 10(A,B), the parent PP (Run 11) is not shown as its MWD overlaps with Run 10, which is PP after melt mixing with 0.5 wt % BPH.

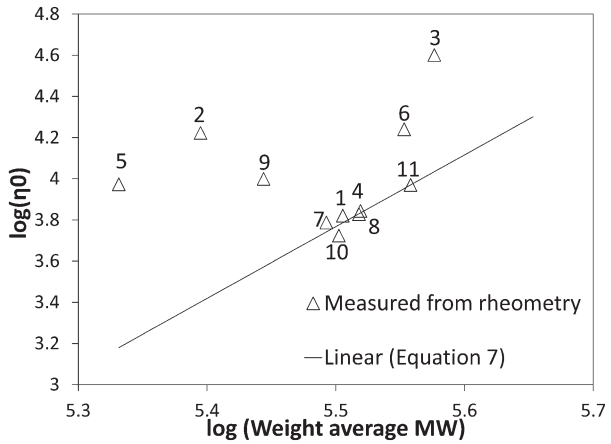

Figure 9. Comparison between calculated (linear reference) and measured η_0 from parallel plate rheometry.

In Figure 10(A), the MWD of Run 1 is slightly shifted toward lower MWDs (relative to that of the reference of Run 10). This shift toward lower MWDs is more significant in Run 2, which is radiated for longer durations. Moreover, the MWD of Run 2 has become significantly broader compared to Run 1 and Run 10 (the reference run). Radiation for 15 min (Run 3) not only results in a broader MWD (compared to Runs 1, 2, and 10) but also shifts the MWD tail to larger MWs. This is in agreement

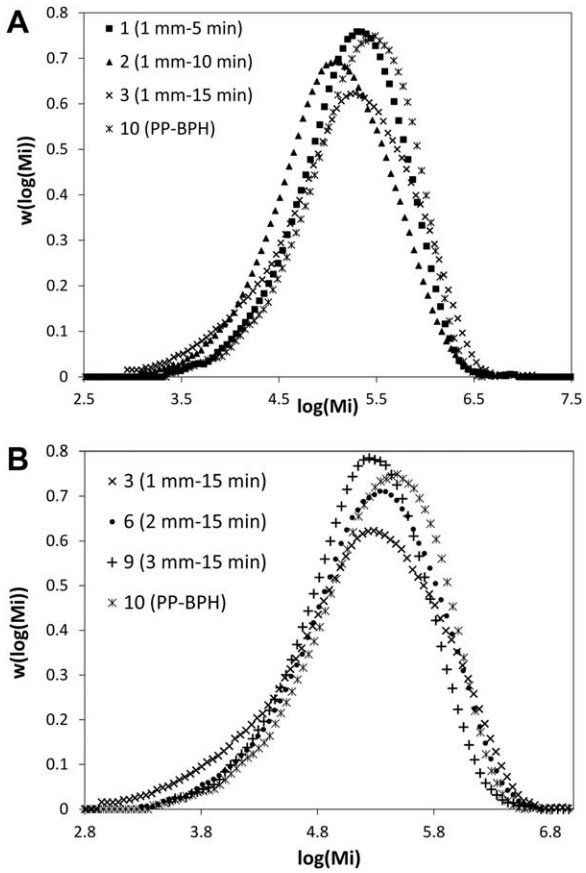

Figure 10. MWDs of the runs (A) with 1 mm thickness at different exposure times to UV and (B) with different thickness after 15 min radiation.

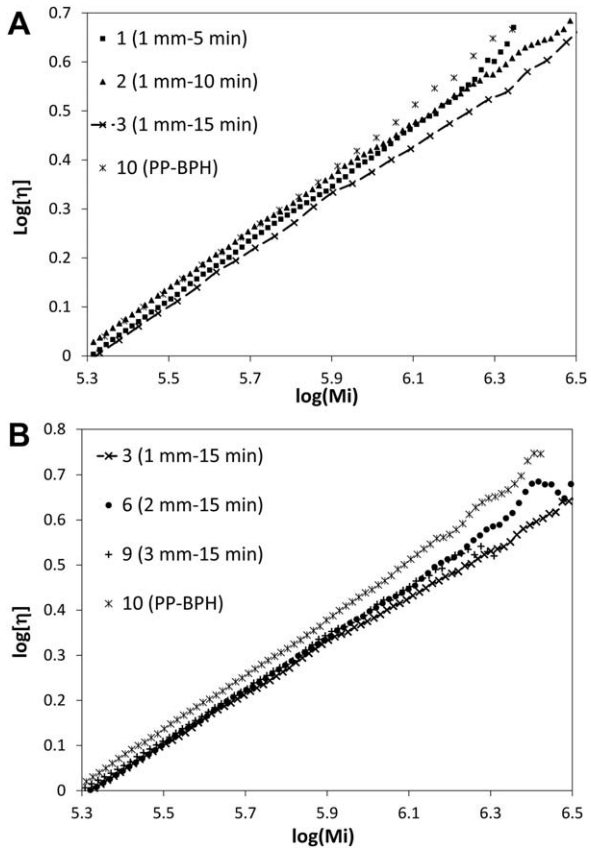

Figure 11. Intrinsic viscosity [η] versus log(Mi) (A) runs with 1 mm thickness at different exposure times to UV and (B) runs with different thickness after 15 min radiation.

with the mechanism of Figure 3, which suggests degradation and LCB happening simultaneously. Hence, an increase in MW happens after long radiation time when the population of LCBs is large enough to compensate for degradation effects on both the MW and MWD.

Figure 10(B) shows the effect of sample thickness on the MWD of the runs that are radiated for 15 min. Comparison between Runs 3, 6, and 9 shows an increase in the population of long chains with a decrease in samples thickness. Consequently, this shifts the distribution toward higher MWs (larger tail in Runs 3 and 6 compared to the parent PP). This is because UV can penetrate thoroughly into the whole depth of the samples, in thinner samples, and hence formation of high MW chains due to LCB is more effective. For Run 9, the distribution becomes narrower and shifts toward lower MWs compared to the reference run (Run 10). This is again due to limitations in UV penetration into the depth of the samples, which results in formation of fewer LCBs in the sample.

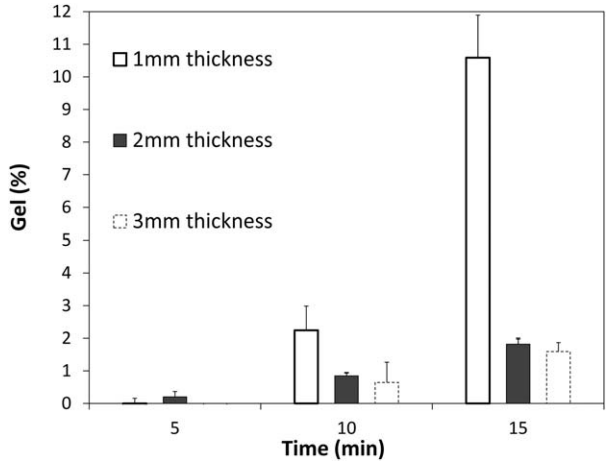

Figure 12. Gel content of the runs with different thickness at different radiation times.

Figure 10(A,B) shows broadening in the MWD of the modified runs (see also the large PDI values of the runs in Table III) toward the high MW end of the distribution. This reflects formation of LCBs. These long chains branches, which are present in the modified runs, increase the number of entanglements in the melt and result in a greater melt strength (larger melt strength of the modified runs was also shown in Ref. 10). These modified PPs can find several processing applications, such as foaming, thermoforming, extrusion coating, film blowing, and blow moulding.[20]

The intrinsic viscosity [η] of the samples was also measured via GPC and compared for different runs. Qualitative comparisons between the obtained curves can serve as an indicator of the molecular structure of the polymers. It is known that formation of LCB in the polymer results in a lower intrinsic viscosity due to the smaller radius of gyration of long chain branched chains. Thus, log [η] versus log (Mi) is linear for a linear polymer with known slope and intercept (Mark–Houwink constants). Mi here represents MW values. However, presence of LCB in the polymer causes deviations from this linear relation by shifting the slope at higher MWs to lower values. As changes in the slope of log [η] − log (Mi) are more significant for thin samples and long radiation times, plots are shown for different radiation times for samples of thickness of 1 mm [Figure 11(A)], and subsequently at 15 min radiation time for different thicknesses [Figure 11(B)]. This way is analogous to the results of Figure 10 (with curve 10 (starred line) representing the reference run). In Figure 11(A), Runs 2 and 3 shows a change in their slope to lower intrinsic viscosities. This change is more pronounced in the slope of Run 3 at MW values of about 790 kg/mol (log (Mi) values of about 5.89). Figure 11(B) shows the intrinsic viscosity of the runs with different thicknesses but with the same radiation time (15 min of radiation). As the thickness of the samples decreases, the deviation from the linear reference becomes clearer (and hence, the presence of LCB).

Effect on Gel Content

To investigate the presence of gel (due to CL) in each run, extraction experiments were carried out. The results from these measurements are summarized in Figure 12. The parent PP (Run 11) and PP after melt mixing with BPH (Run 10) are not shown in Figure 12 since there was no gel found in these samples.

Figure 12 shows that after 5 min radiation almost no gel was detected in the runs and only after 10 min from the onset of radiation significant formation of gel was detected. Increases in

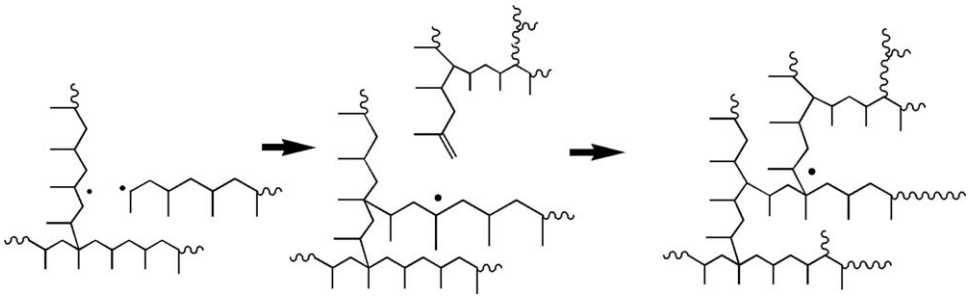

Figure 13. Schematic of mechanism that leads to crosslinking of long chain branched polymers.

radiation time cause larger percentage of CL in the samples with the same thickness. Moreover, decrease in the thickness increases the percentage of gel in the runs. An increase in gel content upon increasing radiation time is more significant at low thicknesses. This is the same trend that was observed in rheological properties earlier.

Formation of gel in the samples might be due to addition of more branches to the chains that are already long chain branched, which may result in formation of network structures. Figure 13 explains this mechanism. These reactions are probable since long chain branched chains have more repeating units and they are statistically more favored to undergo hydrogen abstraction again.

The amount of gel content of the runs was analyzed statistically. As expected, the two-factor interaction (the thickness-time interaction) was found significant.

Figure 14 shows the effect of the thickness-time interaction on the percent gel in the samples. As expected from the previous effects on viscoelastic properties and MW, an increase in thickness at constant radiation time results in lower gel content in the samples. This effect is more pronounced after 15 min of radiation.

CONCLUSIONS

PP has been modified using 0.5 wt % BPH as photoinitiator and UV radiation to introduce LCB to its structure. The effects of radiation time and thickness of samples were investigated simultaneously using three-level factorial experiments. Both factors and their interaction were found to significantly affect the rheological properties, such as η_0, λ, PI, and ModSep, the molecular properties (MW and MWD), and, finally, gel content. ER and the shear thinning index depended on radiation time and thickness but seemed independent of the interaction.

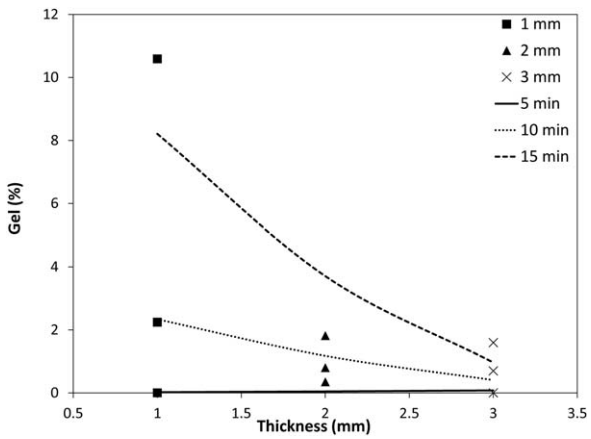

Figure 14. Effect of the time-thickness interaction on gel content.

Both an increase in radiation time and a decrease in thickness of the samples result in a broader relaxation spectrum and larger η_0, λ, and ER, and more shear thinning behavior (smaller n). Conversely, at the same radiation time, thicker samples have lower η_0, λ, and ER, and larger n. Moreover, thick samples are less sensitive to changes in radiation times. Broadening of the relaxation spectrum with increasing radiation time was observed after longer radiation times for thicker samples (2 and 3 mm) compared to 1 mm samples.

The MW and MWD data show that an increase in radiation time and a decrease in sample thickness result in an increase in MW and broadening of MWD. The same trends were observed for the gel content of the samples. Thinner samples which were irradiated for longer durations showed greater gel content than thick samples which were radiated for shorter durations. Lower gel content and lower MW of the thick samples were attributed to limitations in UV penetration depth, which causes inhomogeneities in the formation of LCB throughout the sample.

ACKNOWLEDGMENTS

The authors gratefully acknowledge financial support from the Natural Sciences and Engineering Research Council (NSERC) of Canada, and the Canada Research Chair (CRC) program. Many thanks go to Dr. Dan Bugada and LyondellBasell Company, Cincinnati, Ohio, USA, for providing polypropylene resins for this study.

REFERENCES

1. Tzoganakis, C.; Vlachopoulos, J.; Hamielec, A. *Polym. Eng. Sci.* **1988**, *28*, 170.
2. Auhl, D.; Stange, J.; Münstedt, H.; Krause, B.; Voigt, D.; Lederer, A.; Lappan, U.; Lunkwitz, K. *Macromolecules* **2004**, *37*, 9465.
3. Auhl, D.; Stadler, F. J.; Münstedt, H. *Rheol. Acta* **2012**, *51*, 979.
4. Kim, K. J.; Ok, Y. S.; Kim, B. K. *Adv. Polym. Sci.* **1993**, *28*, 263.

5. Zamotaev, P.; Shibirin, E.; Nogellova, Z. *Polym. Degrad. Stab.* **1995**, *47*, 93.
6. Parent, J. S.; Bodsworth, A.; Sengupta, S. S.; Kontopoulou, M.; Chaudhary, B. I.; Poche, D.; Cousteaux, S. *Polymer* **2009**, *50*, 85.
7. Lugão, A. B.; Cardoso, E. C. L.; Lima, L. F. C. P.; Hustzler, B.; Tokumoto, S. *Nucl. Instrum. Methods Phys. Res. B* **2003**, *208*, 252.
8. Amintowlieh, Y.; Tzoganakis, C.; Penlidis, A. U.S. *Provisional Pat Appl., 61/995,627, April 16*, **2014**.
9. Kukaleva, N.; Stoll, K.; Santi, M. U.S. *Pat. Appl. 0136,931, June 9*, **2011**.
10. Amintowlieh, Y.; Tzoganakis, C.; Hatzikiriakos S. G.; Penlidis, A. *Polym. Degrad. Stab.* **2014**, *104*, 1.
11. He, G.; Tzoganakis, C. *Polym. Eng. Sci.* **2011**, *51*, 151.
12. Chen, Y. L.; Rånby, B. *J. Polym. Sci. A Polym. Chem.* **1989**, *27*, 4077.
13. Tian, J.; Yu, W.; Zhou, C. *Polymer* **2006**, *47*, 7962.
14. Shroff, R.; Mavridis, H. *J. Appl. Polym. Sci.* **1995**, *57*, 1605.
15. Dealy, J. M.; Dealy, J. M. Melt Rheology and its Role in Plastics Processing: Theory and Applications; Van Nostrand Reinhold: New York, **1990**, p 64.
16. Krause, B.; Voigt, D.; Lederer, A.; Auhl, D.; Munstedt, H. *J. Chromatogr. A* **2004**, *1056*, 217.
17. Gabriel, C.; Münstedt, H. *Rheol. Acta* **2002**, *41*, 232.
18. Langston, J. A. Synthesis and Characterization of Long Chain Branched Isotactic Polypropylene Via Metallocene Catalyst and T-Reagent. PhD Thesis, Pennsylvania State University, December **2007**.
19. Wood-Adams, P. M.; Dealy, J. M.; Willem deGroot, A.; Redwine, O. D. *Macromolecules* **2000**, *33*, 7489.
20. Gotsis, A.; Zeevenhoven, B.; Hogt, A. *Polym. Eng. Sci.* **2004**, *44*, 973.